

## Grafted NiO on natural olivine for dry reforming of methane

To cite this article: C Courson *et al* 2002 *Sci. Technol. Adv. Mater.* **3** 271

View the [article online](#) for updates and enhancements.

### You may also like

- [Geoengineering impact of open ocean dissolution of olivine on atmospheric CO<sub>2</sub>, surface ocean pH and marine biology](#)  
Peter Köhler, Jesse F Abrams, Christoph Völker et al.
- [Iron fertilisation and century-scale effects of open ocean dissolution of olivine in a simulated CO<sub>2</sub> removal experiment](#)  
Judith Hauck, Peter Köhler, Dieter Wolf-Gladrow et al.
- [The Early Solar System Abundance of Iron-60: New Constraints from Chondritic Silicates](#)  
János Kodolányi, Peter Hoppe, Christian Vollmer et al.



ELSEVIER

Science and Technology of Advanced Materials 3 (2002) 271–282

SCIENCE AND  
TECHNOLOGY OF  
ADVANCED  
MATERIALS[www.elsevier.com/locate/stam](http://www.elsevier.com/locate/stam)

# Grafted NiO on natural olivine for dry reforming of methane

C. Courson, L. Udron, C. Petit\*, A. Kiennemann

Laboratoire des Matériaux, Surface et Procédés pour la Catalyse, UMR 7515, ECPM 25 Ecole Européenne de Chimie Polymères et Matériaux,  
25 rue Becquerel, 67087 Strasbourg Cedex 2, France

Received 5 October 2001; revised 7 January 2002; accepted 6 February 2002

## Abstract

Natural olivine is used for gasification of biomass in a fluidised bed. Characterisations by X-ray diffraction and electron microscopies (SEM and TEM) have proved the presence of a  $(\text{Mg,Fe})_2\text{SiO}_4$  structure (Mg/Fe ratio: 9/1) with a rather broad distribution in elemental composition. Temperature programmed reduction has revealed equally the presence of iron oxides outside of this structure. The nature of free iron oxides can be both modified by increasing the temperature of calcination and confirmed by measurements of magnetism.

The introduction of nickel oxide upon natural olivine is obtained by impregnation with a nitrate salt. The type of interaction of nickel oxide with olivine is different depending upon the preparation method and the calcination temperature. For calcination at 1100 °C, the effects of the amount of NiO and the number of impregnation have been studied. At a high temperature of calcination (1400 °C), NiO is integrated into the olivine structure and the amount of free iron increases. Integrated NiO on olivine is non-reducible, resulting in an inactive catalyst. At lower calcination temperatures grafted NiO is formed, a species which is reduced under catalytic test conditions without aggregation of particles. A single impregnation of nickel (5.5 wt% of NiO) gives a stable catalyst activated directly under reaction conditions ( $\text{CH}_4 + \text{CO}_2$ ) yielding 96% CO and 76%  $\text{H}_2$ . Catalysts with lower amounts of NiO or a double impregnation of nickel salt lead to a less stable system.

Analysis reveals that no change in olivine structure nor size of nickel deposit occurs under test conditions. Equally there are no carbon deposits formed on these catalysts. A model of the evolution of each catalytic system arising from the different preparation methods is proposed. The observed deactivation of such catalysts is attributed to the increase in the amount of free iron, which favours the oxidative properties of the catalytic system. © 2002 Elsevier Science Ltd. All rights reserved.

**Keywords:** Biomass; Olivine; Perovskite; Syngas; Nickel

## 1. Introduction

Among renewable energy resources, biomass appears to be full of promise for an industrial application [1]. Certain devices are devoted to biomass gasification to produce gaseous hydrocarbons or a  $\text{CO} + \text{H}_2$  mixture, the most useful reaction intermediate for the obtention of basic organic compounds or hydrogen [2]. Fluidised bed gasification is the most appropriate method by which a maximum of valorisable products might be attained [3]. An abrasion resistant basic oxide, having a density similar to that of the biomass can be added to optimise the gasification [4], while a catalyst can be introduced to favour the re-formation of light hydrocarbons. From technical and economical considerations, nickel-containing catalysts appear to be the most appropriate choice. The complexity of the problem lies in the conception of an effective nickel-containing catalytic

system, consistent with the requirements of fluidised bed biomass gasification. The results of tests undertaken previously have revealed that the characteristics of a natural olivine (hardness, density, and basicity) would be of particular interest in respect of this application. Active phase-support interactions affect the dispersion of transition metals and the catalytic activity of the catalysts prepared from them [5,6]. Che and Bonneviot [7] have developed a two-step preparation method capable of controlling the particle size of an  $\text{Ni/SiO}_2$  catalyst. The nucleation step gave nickel oxide nuclei in strong interaction with the support; thereby the impregnation step effectively yielded a nickel reservoir [8].

The present study deals with the nickel oxide-support interaction on natural olivine and its reducibility. The effects of the active phase composition (Ni and/or NiO) are considered in relation to the catalytic properties in the dry reforming of methane ( $\text{CH}_4 + \text{CO}_2$ ). Based upon analytical interpretation, the nature of the type of interaction between the nickel species and the support is proposed.

\* Corresponding author. Tel.: +33-388-1369-76; fax: +33-388-1369-75.  
E-mail address: [petitc@ecpm.u-strasbg.fr](mailto:petitc@ecpm.u-strasbg.fr) (C. Petit).

## 2. Experimental

### 2.1. Preparation of Ni/olivine catalysts

Natural olivine is mined in Austria and has been produced for this study. Thanks to our EU project partners. The Magnolithe manufacturing process delivers the material following crushing and sieving to obtain defined particle sizes (400 and 600  $\mu\text{m}$ ). The fraction between 315 and 400  $\mu\text{m}$  is only 6 wt% and was studied in its natural state or following calcination in air through various temperatures between 750 and 1400  $^{\circ}\text{C}$  over 4 h with a increasing temperature ramp of 3  $^{\circ}\text{C min}^{-1}$ . The Ni/olivine catalyst was prepared by impregnation of the olivine by an aqueous solution of  $\text{Ni}(\text{NO}_3)_2 \cdot 6\text{H}_2\text{O}$  in excess (1 g in 7.5 ml of water). After the evaporation of the excess water, the material was calcined through the same range of temperatures as the sequence previously described, attained via the same ramp. Two catalysts were made in this way possessing 3.5 and 5.5 wt% of NiO, respectively. A third catalyst (5.5 wt% of NiO) was prepared by incorporating a second impregnation of the nickel nitrate salt in excess on the 3.5 wt% of NiO sample calcined at 1100  $^{\circ}\text{C}$  and calcined again at 1100  $^{\circ}\text{C}$  over 4 h with an increasing temperature ramp of 3  $^{\circ}\text{C min}^{-1}$ .

### 2.2. Characterisation methods

The olivine and the resulting catalytic systems were characterised by powder X-ray diffraction (XRD Siemens D500 TT diffractometer,  $\text{Cu K}_{\alpha}$  radiation), scanning electron microscopy (SEM, JEOL JSM 840 microscope) and transmission electron microscopy (TEM TOPCON EM-002 B). For the TEM analyses, the samples were ground, deposited upon a Cu grid and covered by a perforated carbon membrane. The statistical distribution of Si, Mg, Fe and Ni was obtained by microanalysis with a broad analysis window ( $\Phi = 200 \text{ nm}$ ). Elementary analysis enabled the evaluation of the correction coefficients to be applied to the values obtained by TEM analysis. The distribution over different areas of the samples was obtained using a small analysis window ( $\Phi = 14 \text{ nm}$ ) and led to the determination of the homogeneity of the samples [9].

### 2.3. Temperature programmed reduction

The temperature programmed reduction (TPR) studies were performed in a quartz U-shaped tube (6.6 mm inner diameter) with 200 mg of catalyst. An  $\text{H}_2$  (0.12  $\text{nl h}^{-1}$ ) + Ar (3  $\text{nl h}^{-1}$ ) mixture flows through the reactor heated from room temperature up to 910  $^{\circ}\text{C}$  with a 15  $^{\circ}\text{C min}^{-1}$  increasing temperature ramp. A thermal conductivity detector analysed the effluent gas following passage of a water trap and enabled the quantification of the hydrogen consumption. A calibration of hydrogen was made by injection of a series of pulses (0.5 ml each). The total

amount of hydrogen consumption was determined by comparison of the different surfaces but the instantaneous data could not be deduced.

### 2.4. Catalytic tests

Catalyst (400 mg) were placed in a quartz U-shaped tube (6.6 mm inner diameter reactor). The catalyst was tested at atmospheric pressure in dry reforming of methane ( $\text{CH}_4 + \text{CO}_2$ ) under the following standard conditions: Argon (2.4  $\text{nl h}^{-1}$ ),  $\text{CH}_4$  (0.3  $\text{nl h}^{-1}$ ) and  $\text{CO}_2$  (0.3  $\text{nl h}^{-1}$ ) flows provided a  $\text{CH}_4/\text{CO}_2$  stoichiometric of 1. The flows were controlled by mass flowmeters.

The outlet gas was analysed simultaneously by two gas chromatographs equipped with TCD. The first registered both the amounts of  $\text{CH}_4$ ,  $\text{CO}_2$  remaining and of produced CO separated on a carbosieve SII column (3 m; 80–100 mesh; He: 25  $\text{ml min}^{-1}$ ); the second quantified CO and  $\text{H}_2$  production separated on a molecular sieve (2 m; 5  $\text{\AA}$ ; 80–100 mesh; Ar: 18  $\text{ml min}^{-1}$ ).

The initial  $\text{CH}_4$  and  $\text{CO}_2$  data were measured by by-pass analysis. The catalytic test of the samples was started up, without reduction pre-treatment, under the gas flow mixture described.

The temperature program comprised an initial treatment followed by three consecutive cycles. The initial treatment consisted of a temperature increase from 25 to 500  $^{\circ}\text{C}$  with a gradient of 10  $^{\circ}\text{C min}^{-1}$ . During this step no gas formation occurred upon any catalyst. During the first cycle the temperature was increased from 500 to 800  $^{\circ}\text{C}$  (rate of 3  $^{\circ}\text{C min}^{-1}$ ), then maintained constant during 3 or 4 h before cooling to 500  $^{\circ}\text{C}$ . The catalyst was kept overnight at this latter temperature in an atmosphere of argon. The second cycle resembled the first while the third cycle was limited to a temperature increase up to 800  $^{\circ}\text{C}$  followed by a cooling. During the program, the products were analysed every 20 min. From the amounts of  $\text{CH}_4$  or  $\text{CO}_2$  remaining conversions could be calculated as follows:

$$\text{Conversion (of product } i) = \frac{(C_{i,i} - C_{i,r})}{C_{i,i}} \times 100 \quad (1)$$

$C_{i,i}$  is the amount of product  $i$  ( $\text{CH}_4$  or  $\text{CO}_2$ ) introduced,  $C_{i,r}$  is the amount of product  $i$  ( $\text{CH}_4$  or  $\text{CO}_2$ ) remaining.

Given the following reaction (2), the CO and  $\text{H}_2$  molar yields can be deduced.



$$\text{H}_2 \text{ yield (\%)} = \frac{\text{number of H}_2 \text{ moles formed}}{\text{number of CH}_4 \text{ moles introduced}} \times \frac{100}{2}$$

$$\text{CO yield (\%)} = \frac{\text{number of CO moles formed}}{\text{number of CH}_4 \text{ moles introduced}} \times 100$$

If the ratio  $\text{CO}/\text{H}_2$  is different from 1, a second reaction

occurs



### 3. Results

#### 3.1. Study of the natural olivine

The composition of the natural olivine determined by atomic absorption (30.5 wt% of Mg, 7.1 wt% of Fe and 19.6 wt% of Si) is near  $(\text{Mg}_{0.9}\text{Fe}_{0.08})_2\text{SiO}_4$  with a slight excess of iron present as free iron oxide (0.7 wt% Fe). The mineral already contains small amounts of nickel as well as Ca, Al and Cr (lower than 0.2 wt% each). The specific surface area is very small ( $< 1 \text{ m}^2 \text{ g}^{-1}$ ). The XRD spectrum of the olivine is close to that of the  $\text{Mg}_2\text{SiO}_4$  forsterite [10]. In fact, the crystalline structures of  $\text{Fe}_2\text{SiO}_4$  and  $\text{Mg}_2\text{SiO}_4$  are very similar and the lattice parameters are almost equal. Following its use in the experiments olivine presents XRD spectra which reveals changes in the intensities of the different planes which are dependent upon the samples examined. Only a small contribution of the  $(\text{Mg,Fe})\text{SiO}_3$  phase is observed at  $2\theta = 28.2^\circ$  [11] and iron oxide. After calcination of the olivine at  $1100^\circ\text{C}$ , crystalline phases

similar to those of the natural mineral are observed with almost no change in the line positions and overall intensities. The calcination at  $1400^\circ\text{C}$  gives an increasing of the strongest lines of the secondary phases:  $(\text{Mg,Fe})\text{SiO}_3$  and  $\text{Fe}_3\text{O}_4$ . Transition electron microscopy (TEM) and energy dispersive spectroscopy (EDS) analyses were performed on different areas of the natural olivine sample with both a narrow and broad analysis window. A photograph and the corresponding elemental distribution are shown in Fig. 1. The data obtained by narrow field analyses were compared themselves and with the mean values estimated from the broad window examination used as references. Other areas were studied and 7 out of 11 of them proved to be close to the mean values (Si 38 wt%  $\pm$  4, Mg 40 wt%  $\pm$  4, Fe 17 wt%  $\pm$  6). Three of them presented a larger amount of iron (Si 1–18 wt%, Mg 2–18 wt% and Fe 63–92 wt%). XRD and TEM analyses indicated that the natural olivine is mainly composed of one crystalline phase with some heterogeneity in the distribution of elements and particles of free iron oxides. The colour of the sample changes as a function of the temperature of calcination. The natural olivine has a brown colour and the magnetic studies suggest the presence of magnetic  $\text{Fe}_3\text{O}_4$ . Knowing that the colour of olivine is due to free iron oxide, these species comprise a mixture of  $\text{Fe}_2\text{O}_3 \cdot 3\text{H}_2\text{O}$  and a small contribution

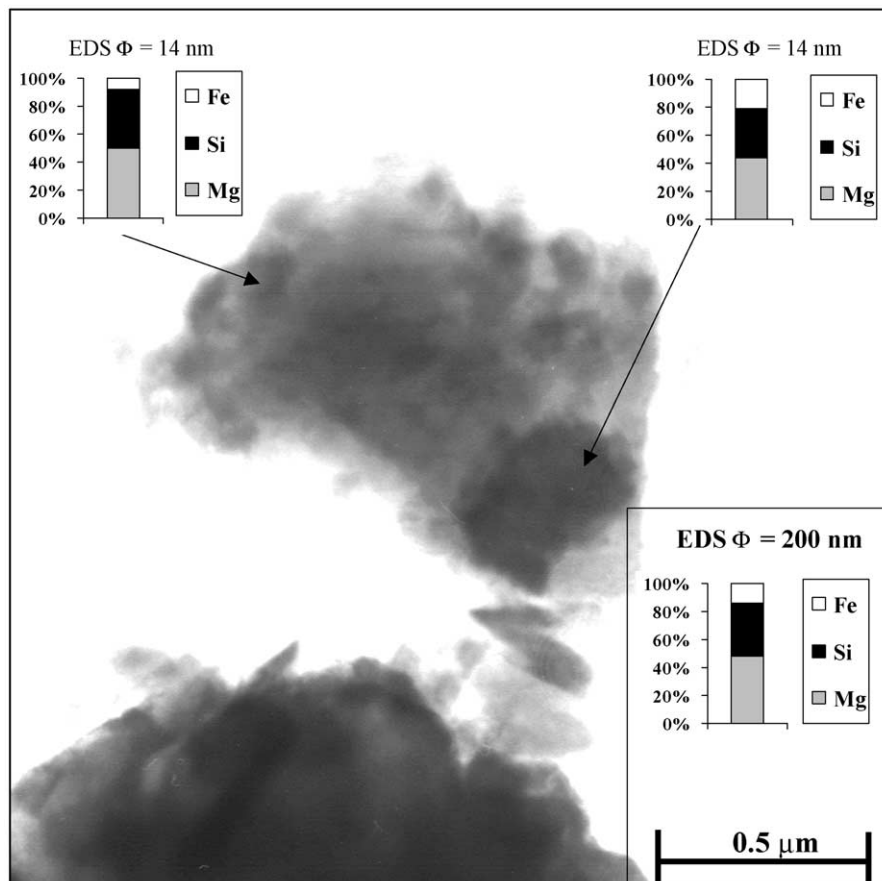


Fig. 1. TEM and EDS analysis of natural olivine before calcination.

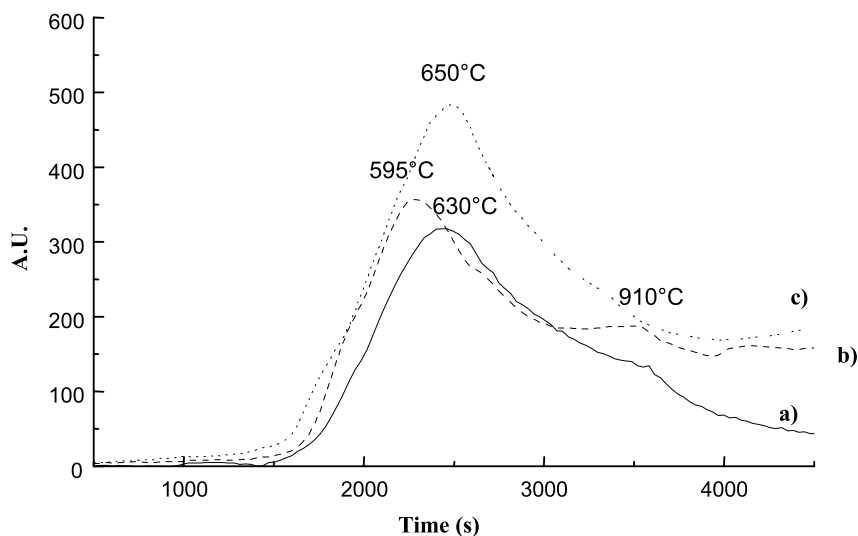


Fig. 2. TPR of (a) natural olivine (—), (b) olivine calcined at 1100 °C (---), and (c) olivine calcined at 1400 °C (···).

of  $\text{Fe}_3\text{O}_4$  for the natural olivine before calcination. Calcination at 1100 °C led to the olivine taking a red-brown colour in agreement with a  $\text{Fe}_2\text{O}_3$  species formation while the reduction of the magnetic qualities of  $\text{Fe}_3\text{O}_4$  are indicative of decrease in the presence of this oxide. Higher temperature calcination (1400 °C) yielded a black colour. According to the phase diagram [12] and the magnetic measurement, the free iron oxide is partially reduced from  $\text{Fe}_2\text{O}_3$  to the oxides mixture ( $\text{FeO}$ ,  $\text{Fe}_2\text{O}_3$ ) or to the magnetic species ( $\text{Fe}_3\text{O}_4$ ). The sub-oxides are able to trap water easily.

TPR profiles for olivine calcined at different temperatures are shown in Fig. 2. The temperature was increased with a rate of  $15\text{ °C min}^{-1}$  (from 25 °C) up to 910 °C where it was maintained. The curves define clearly the two regions, the increasing in temperature and the isothermal one at 910 °C. For natural olivine (line a) a reduction peak is observed around 630 °C as well as a drift at 910 °C. The first peak is attributed to the reduction of the 'extra framework' iron oxide of the natural olivine, as detected by TEM. Earlier work [13] in our laboratory reported that iron oxides inserted in a well-defined structure can only be reduced at temperatures higher than 900 °C. The XRD spectrum of the sample after TPR shows that while the olivine phase is maintained a metallic iron phase also appears. According to the calibration presented in Section 2, the consumption of hydrogen for this sample corresponds to the reduction of 3 wt% of  $\text{Fe}_2\text{O}_3$  approximately. The drift observed at 910 °C corresponds to the beginning of the reduction of iron oxides inserted into the olivine. After calcination at 1100 °C (line b) and 1400 °C (line c), the profiles of the catalysts also present two peaks. As shown for natural olivine, the partial reduction of the iron oxide within olivine is attained at 910 °C for the calcined olivine. The difference in the profiles is the reduction of the different nature of free iron oxides in function of the initial treatment. Without treatment, the free iron oxide on olivine is identified as  $\text{Fe}_2\text{O}_3 \cdot 3\text{H}_2\text{O}$ . After

calcination at 1100 °C, the free iron is mainly anhydrous  $\text{Fe}_2\text{O}_3$  given a reduction at a lower temperature (595 °C) in comparison with iron oxide into natural olivine (630 °C). The crystalline water delays the reduction temperature of the iron oxide by the limitation of the hydrogen approach. The TPR of the olivine calcined at 1100 °C, having undergone a preliminary treatment by addition of water, presents a peak at 630 °C, confirms this effect of water on the TPR profile.

Olivine calcined at 1400 °C presents a peak at 650 °C which corresponds to the reduction of  $\text{Fe}_3\text{O}_4$  shown by XRD. The consumption of hydrogen is higher than that obtained with the natural olivine. SEM analysis confirms the presence of more iron rich areas after calcination [14]. Profile of the reduction of the iron within olivine is also modified as if calcination help the extraction of iron oxide.

### 3.2. Study of nickel catalysts deposited on olivine

Four catalysts were prepared by impregnation of a nickel nitrate solution upon olivine. As described in Section 2, the parameters under study were the calcination temperature (750, 900, 1100 and 1400 °C), the amount of NiO deposited and the number of impregnation. Five of the catalysts employed were prepared via a single impregnation of nickel nitrate: 3.5 wt% NiO on olivine calcined at 750, 900, 1100 and 1400 °C, 5.5 wt% NiO on olivine calcined at 1100 °C. Finally, a two-step impregnation method permitted to obtain a 5.5 wt% NiO on olivine calcined at 1100 °C.

XRD spectra of the catalysts were compared with those of natural olivine calcined at the same temperature. The results of olivine and NiO upon olivine calcined at 1100 °C is shown in Fig. 3. XRD reveals that the olivine phase is maintained with a slight shift when compared with the JCPDS file of the  $\text{Mg}_2\text{SiO}_4$  reference [10,15]. The peculiarities of the natural olivine were observed: variation of the relative intensity of the lines with the sampling and a

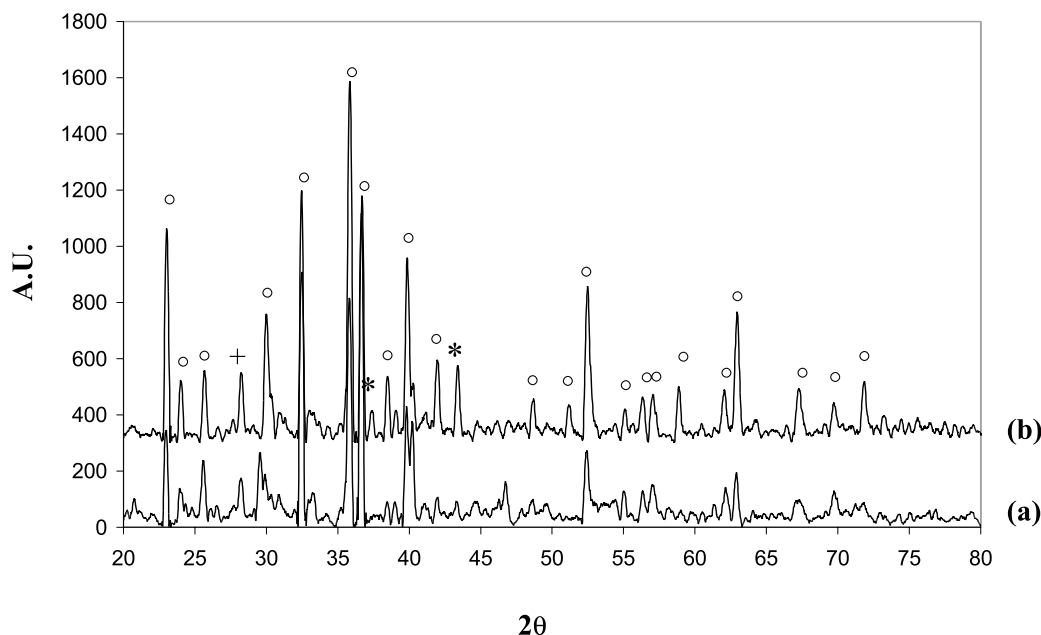


Fig. 3. XRD spectra of (a) olivine calcined at 1100 °C, (b) 3.5 wt% NiO/olivine calcined at 1100 °C; Crystalline phases as: (○)  $\text{Mg}_2\text{SiO}_4$ , (+)  $(\text{Mg,Fe})\text{SiO}_3$ , (\* ) NiO.

small increase of the crystallisation with the calcination treatment. These observations were made for all the samples, without influence of preparation and calcination mode.

The results of the formation of nickel oxide species are shown in Fig. 4 for the areas are situated at  $2\theta$  between 39 and 56°. The cubic NiO phase gives two lines at 37.5 and 43.5° [16]. For temperatures of calcination at 750 (line a), 900 (line b) and 1100 °C (line c), the NiO phase has been observed. They indicate the presence of aggregates of large size. The X-ray diffractogram of the catalyst prepared by double impregnation is similar to that obtained in applying a single impregnation with 5.5 wt% of NiO and calcination at 1100 °C. The characteristic lines of the cubic NiO phase

disappear following calcination of the sample at 1400 °C (line d). This indicates a decrease in size of the nickel-containing particles and/or an insertion into the olivine structure. SEM micrographs of the catalysts obtained under the different conditions were performed. After calcination at 750 and 900 °C, a deposit of almost uniform spherical grains of size range 0.1–0.2  $\mu\text{m}$  is observed which masks completely the surface of the support (Fig. 5 for catalyst at 900 °C). These grains are not present on the micrographs of pure olivine and are consequently attributed to nickel oxide deposits.

Increasing the calcination temperature to 1100 °C leads to a less homogeneous definition of the sample. Some areas are similar to those obtained with NiO on olivine calcined at

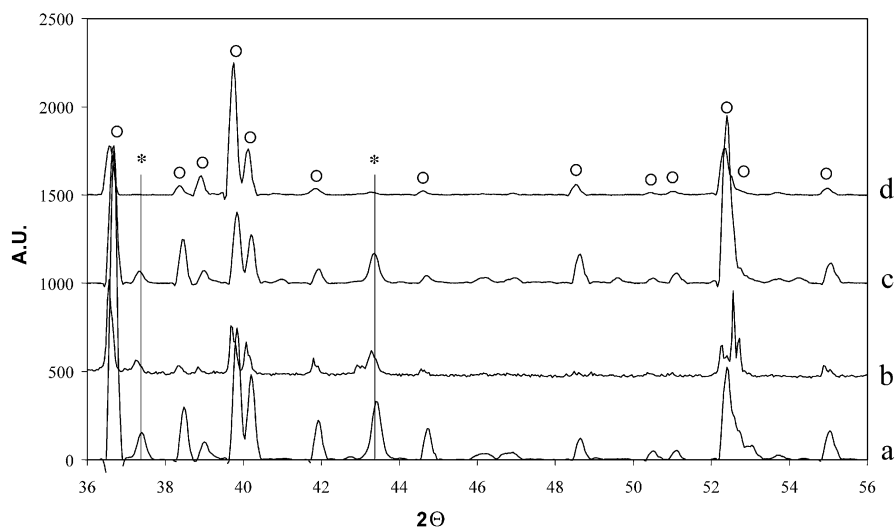


Fig. 4. XRD spectra of 3.5 wt% NiO/olivine calcined at (a) 750, (b) 900, (c) 1100 and (d) 1400 °C; Crystalline phases as: (○)  $\text{Mg}_2\text{SiO}_4$ , (\* ) NiO.

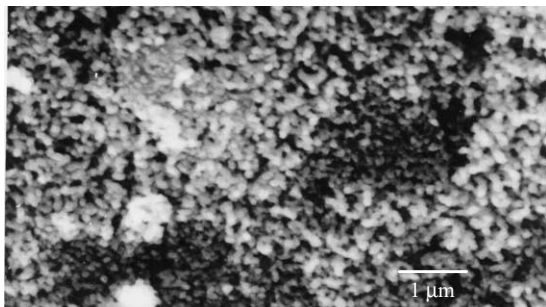


Fig. 5. SEM analysis of 5.5 wt% NiO/olivine calcined at 900 °C.

lower temperature with deposited particles of the same size. Other regions show a thinner coverage of nickel oxide with larger deposited grains (1 μm). Finally, in some areas, the smooth support is observed and the formation of defined plans begins. The catalysts were sieved after impregnation for particles sizes between 250 and 600 μm before catalytic tests. By EDS analysis, the fraction with particles smaller than 250 μm contained a very small amount of silica (lower than 2%) and a modest contribution of Mg (lower than 13%). This is an indication that this fraction of catalyst corresponds to the concentration of nickel oxides which have left the olivine. The analysis conveys information regarding the nature and the morphology of the nickel particles formed on the surface of the catalysts. TEM analyses, shown in Fig. 6, can be considered being an expression of the nature of the particles. The first is formed by pure nickel oxide. The bulk NiO is obtained after heating and nitrate salt decomposition. The morphology of the larger particles corresponds to the growth of smaller ones as described by Yang et al. [8]. As previously reported, the distribution of free iron oxides is wider in the fraction of olivine of smaller size from the original sieving of the mineral. The second one is formed by homogeneous Ni–Fe oxide particles due to the interaction of impregnated nickel and free iron oxide species. These observations seem to indicate that nickel on olivine can be present as NiO and Ni–Fe oxides. The most obvious difference between the samples obtained following a second impregnation (5.5 wt% NiO on olivine) and that having received only a single impregnation (3.5 wt% NiO on olivine) is an enhancement in the coverage by the deposit, which is more regularly distributed upon the surface. When the amount of NiO increases the size of nickel particles is greater (almost a ratio of 2).

Calcination at 1400 °C leads to the formation of a very smooth olivine surface similar to that obtained with the natural olivine calcined at the same temperature (Fig. 8). There is, however, a sparse distribution of spherical particles present upon this surface (1 μm).

Transmission electron microscopy and EDS results for different areas of 5.5 wt% NiO on olivine calcined at 1100 °C are shown in Fig. 7. Similar crystallite particles size of 0.1 μm observed by TEM were identified by EDS as nickel oxide. The distribution of elements Mg, Fe, Si reveals

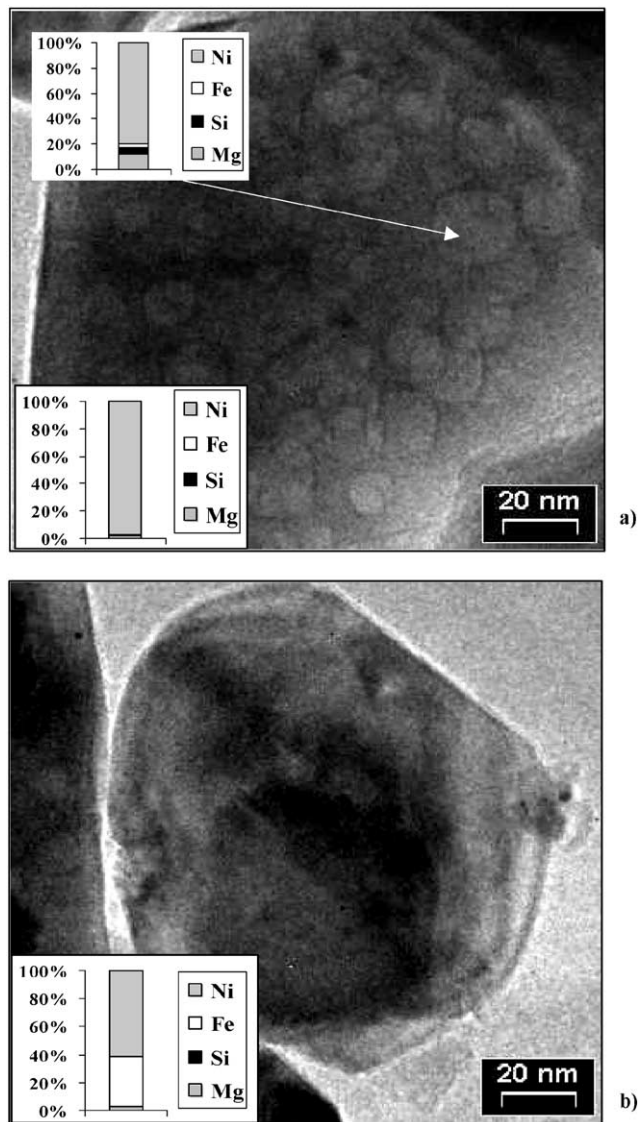


Fig. 6. TEM and EDS ( $\Phi = 14$  nm) analysis of 5.5 wt% NiO/olivine calcined at 1100 °C, sieving under 250 μm (a) area of nickel oxide, (b) area of nickel and iron oxide.

an  $(\text{Mg,Fe})_2\text{SiO}_4$  olivine without noticeable composition changes compared with the natural support alone. After calcination at 1400 °C, the nickel oxide aggregates are no longer observed and the EDS analysis confirms that nickel oxide is integrated into the olivine structure as shown by SEM (Fig. 8).

### 3.3. Catalytic reactivity studies

In order to determine the catalytic activity and the stability of the various catalysts for reforming of light hydrocarbons under conditions presented by biomass pyrolysis, the reaction of reforming dry methane (by  $\text{CO}_2$ ) provides an approximation. Conversion data for consumption of  $\text{CH}_4$  and  $\text{CO}_2$  plus yields of  $\text{CO}$  and  $\text{H}_2$  for the one-step 5.5 wt% NiO/olivine calcined at 1100 °C are shown in

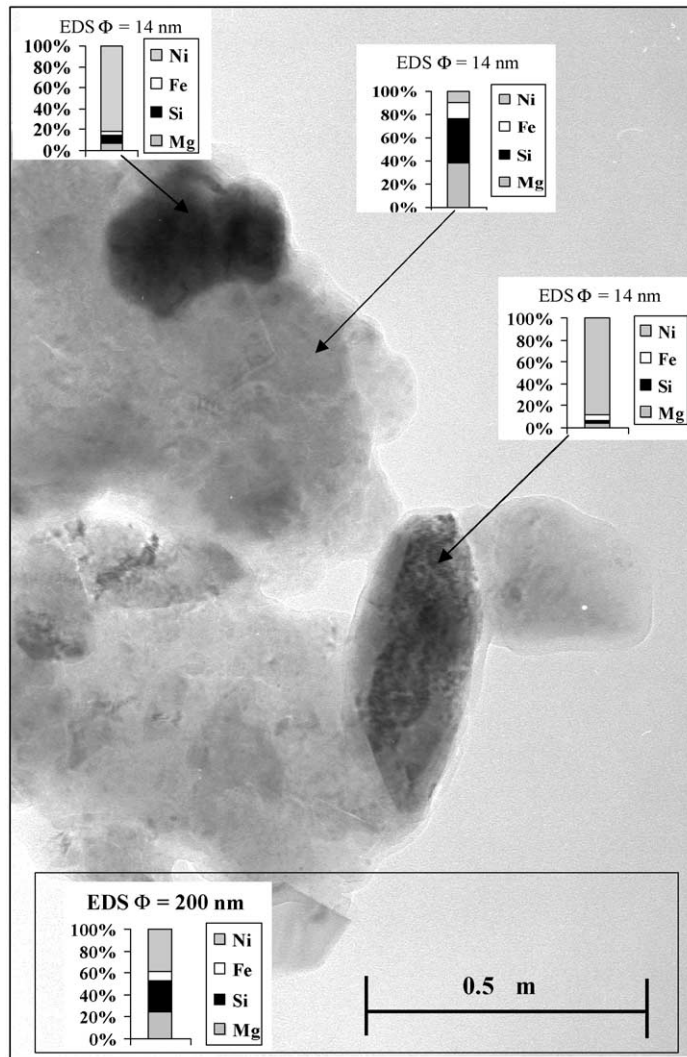


Fig. 7. TEM and EDS analysis of 5.5 wt% NiO/olivine calcined at 1100 °C sieving between 250 and 600 μm.



Fig. 8. SEM analysis of 3.5 wt% NiO/olivine calcined at 1400 °C.

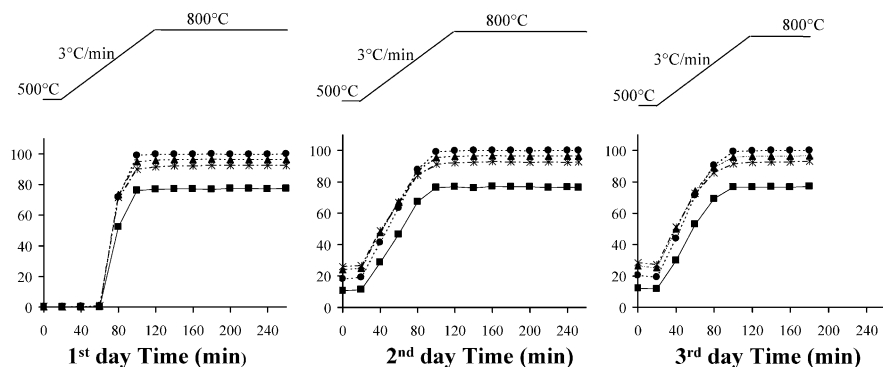


Fig. 9. Activity of 5.5 wt% NiO/olivine calcined at 1100 °C as a function of temperature and time, CH<sub>4</sub>/CO<sub>2</sub> ratio: 1, flow gas: 7.5 nl h<sup>-1</sup> g<sub>cat</sub><sup>-1</sup>. ■— H<sub>2</sub> yield, - -▲- - CO yield, ····●··· CH<sub>4</sub> conversion, - - × - - CO<sub>2</sub> conversion.

Fig. 9. As indicated in Section 2, the catalytic tests were performed without a prior reduction of the catalyst and following a similar program of temperature increase comprising two cycles and a third heating stop. Each test was made during 3 days.

During the first heating ramp (Fig. 9, part a), the activity of the catalyst for CH<sub>4</sub> and CO<sub>2</sub> is initiated around 680 °C. The conversions of both reactants are approaching 70%. They increase with the temperature and are almost complete at 800 °C (99 and 96%, respectively). The distribution of products (CO<sub>2</sub>, CO and H<sub>2</sub>) is constant during the steady state condition. Very high yields of CO and H<sub>2</sub> are observed (96 and 76%, respectively). The stoichiometric ratio CO/H<sub>2</sub> is higher than 1 (1.3), a result which suggests that the principal reaction proposed (CH<sub>4</sub> + CO<sub>2</sub> → 2CO + 2H<sub>2</sub>) is not the sole reaction that occurs.

The second heating ramp (Fig. 9, part b) initiates catalytic activity at a lower temperature compared with its predecessor. In fact, the CH<sub>4</sub> and CO<sub>2</sub> conversions attain a turnover of 20% on immediate contact with the CH<sub>4</sub> + CO<sub>2</sub> gas mixture at 500 °C. The conversions increase in parallel with temperature up to the same high values observed during the first cycle. The CO/H<sub>2</sub> ratio is close to that obtained previously (1.3). The behaviour of the catalyst during the third cycle (Fig. 9, part c) is exactly the same as that during the second one (part b).

In reviewing, the principal modification to the catalytic behaviour is observed between the first heating and the subsequent increases of temperature. At the beginning of the test, nickel is in an oxidised state and need to be reduced. The reduction occurs during the first cycle leading to a yield of similar catalytic results at high temperature for all three cycles. The same behaviour observed during the second and the third ramps indicates that the state of the nickel particles is comparable. During the first cycle, the activation of the catalytic system is enabled by the nickel oxide particle reduction. As shown by TPR, nickel is reduced under these conditions.

A comparison of the activity of the 3.5 wt% NiO

catalysts prepared at different temperatures for CH<sub>4</sub> and CO<sub>2</sub> during the first heating ramp is shown in Fig. 10. The activity of the NiO/olivine calcined at 750 or 900 °C catalyst are initiated at a lower temperature than the catalyst calcined at 1100 °C (at 610 °C) and are increased much more quickly. The conversions of both reactants are the same that NiO/olivine calcined at 1100 °C for a temperature of reaction equal to 750 °C and higher. Thermodynamic equilibrium is obtained at 800 °C under the steady state given the same and very high yields of CO and H<sub>2</sub> (96 and 76%, respectively). The activity of catalyst calcined at 1400 °C is more lower (beginning at 800 °C, low activity at 900 °C).

The reduction depends on the nature of the interaction between the NiO and the olivine. The interaction is less in the case of the catalysts calcined at 750 and 900 °C as shown by the presence of a peak of reduction under hydrogen at 450 °C (TPR not presented). At the beginning of the CH<sub>4</sub>/CO<sub>2</sub> test, nickel oxide is more easy to be reduced and presents a higher activity for the both systems. After a calcination at 1400 °C, as shown previously, the NiO is bonded into the olivine and low reduction is observed, given low catalytic activity.

The results of catalyst ageing during the reforming dry methane are shown in Fig. 11 for the samples 3.5 wt% NiO, 5.5 wt% NiO prepared with one or two-step method. At the beginning of the tests, the conversion of methane is very high (98% at 800 °C) for the three catalysts. Nevertheless for on stream (CH<sub>4</sub> + CO<sub>2</sub>), the activity versus time depends mainly upon the preparation mode.

The best system: the one-step 5.5 wt% NiO on olivine calcined at 1100 °C presents a stable activity (99% CH<sub>4</sub> conversion, 93% CO<sub>2</sub> conversion, 96% CO yield with an H<sub>2</sub>/CO ratio of 0.8) over 200 h of catalytic testing at 800 °C and a 95% CH<sub>4</sub> conversion, almost constant at 750 °C (line a, during the first 100 h).

As shown in Fig. 11, line b, the catalyst obtained by a two-step impregnation has an initial activity similar to that of 5.5 wt% NiO on olivine but this activity decreases sharply to CH<sub>4</sub> and CO<sub>2</sub> activities of 15 and 26%, respectively. The CO yield falls to 22% and the H<sub>2</sub>/CO

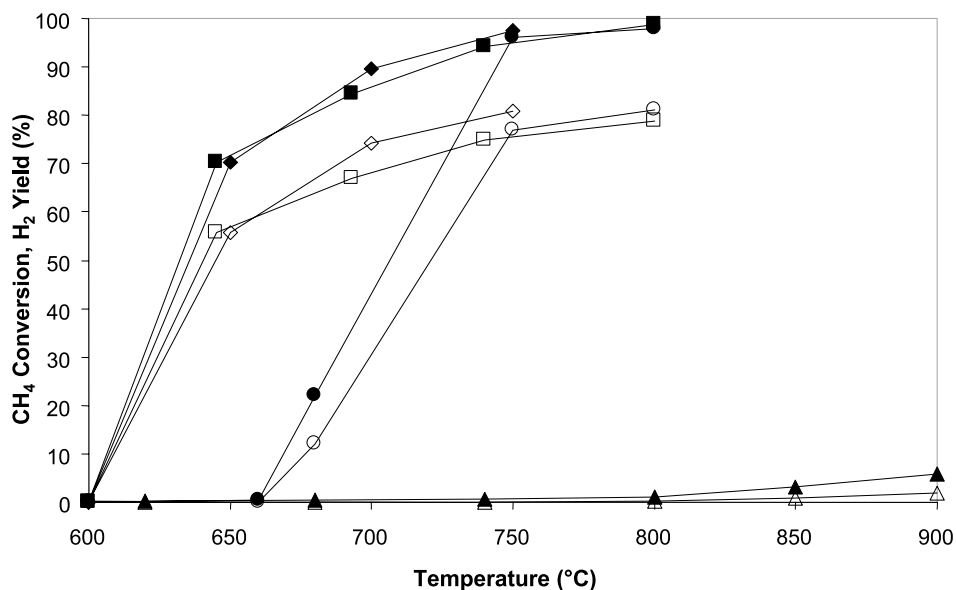


Fig. 10. CH<sub>4</sub> conversion (black symbols) and H<sub>2</sub> yield (open symbols) under the first increase of temperature for 3.5 wt% NiO/olivine as a function of temperature CH<sub>4</sub>/CO<sub>2</sub> ratio: 1, flow gas: 7.5 nl h<sup>-1</sup> g<sub>cat</sub><sup>-1</sup> temperature of calcination at (a) 750 °C (□—), (b) 900 °C (◇—), (c) 1100 °C (○—) and (d) 1400 °C (△—).

ratio tends to 0.6. The difference between the selectivities in CO and H<sub>2</sub> implies that the reverse water–gas shift reaction produces an increasing effect upon this catalyst with ageing. The differences in CH<sub>4</sub> and CO<sub>2</sub> conversions and in yields of CO and H<sub>2</sub> (CO/H<sub>2</sub> ratio > 1) indicate that a second reaction CO<sub>2</sub> + H<sub>2</sub> → CO + H<sub>2</sub>O, known as the reverse water–gas shift reaction occurs. This reaction increases in the presence of iron on the catalyst [17].

On the catalyst having 3.5 wt% of NiO (Fig. 11, line c), the conversion of CH<sub>4</sub> decreases from 98 to 86% following 100 h before stabilising.

The catalysts prepared by a single impregnation maintain

a high activity with time on stream. The behaviour of the sample varies with the amount of NiO: the catalyst prepared with 5.5 wt% of NiO is more stable than that containing 3.5 wt% of NiO.

The efficiency of the 5.5 wt% NiO/olivine catalyst is confirmed by elemental analysis, which reveals that the amount of deposited carbon is low (about 1 wt% of C). A much lower value (0.13 wt% of C) is obtained for the catalyst prepared by the two-step impregnation, which suggests that deactivation cannot be attributed to carbon deposition upon the surface. Equally, it can be proposed that the nature of the nickel oxide particles found upon

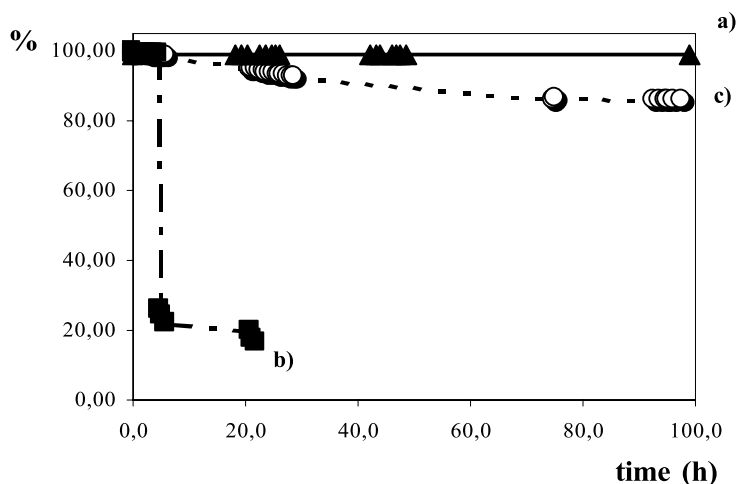


Fig. 11. Ageing of NiO catalysts on olivine calcined at 1100 °C. (a) 5.5 wt% NiO/olivine one step impregnation, (b) 5.5 wt% NiO/olivine two-step impregnation, (c) 3.5 wt% NiO/olivine one step impregnation. CH<sub>4</sub>/CO<sub>2</sub> ratio: 1, flow gas: 3 nl h<sup>-1</sup> g<sub>cat</sub><sup>-1</sup>, temperature test: 800 °C. ...••••• CH<sub>4</sub> conversion.

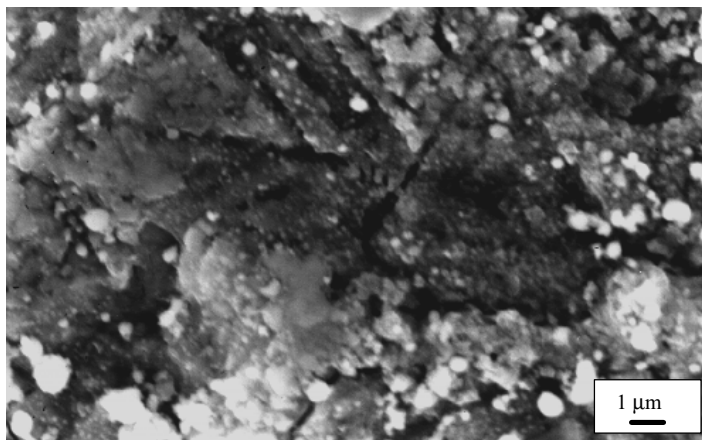


Fig. 12. SEM analysis of 5.5 wt% NiO/olivine one step impregnation, calcined at 1100 °C after test.

the surface of the olivine following the second impregnation is different from those resulting from the previous one which suggests a modification in the type of grafting. This latter point will be discussed in Section 3.4.

### 3.4. Characterisation of nickel on olivine catalysts after test

In order to understand the evolution of the system during the test, the catalysts were characterised following analysis by XRD and SEM. The crystalline phases detected by XRD

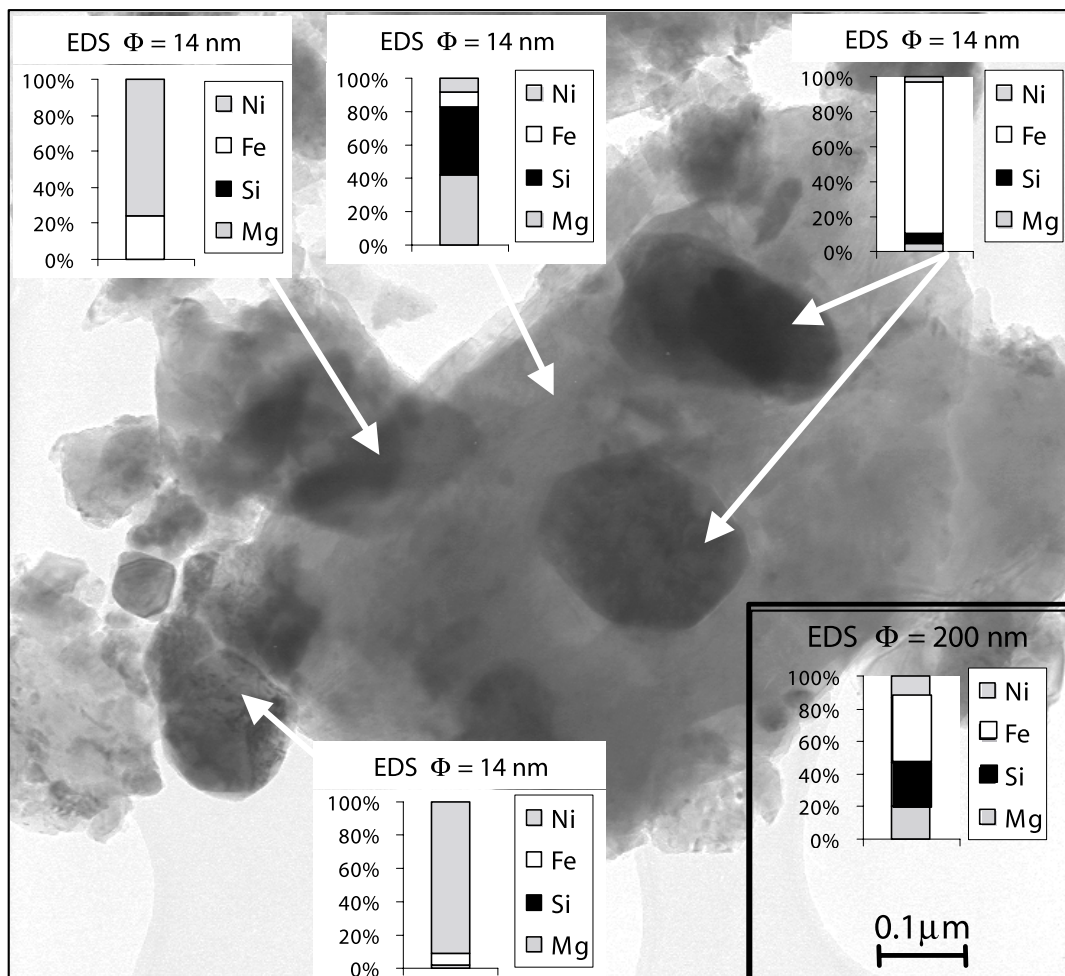


Fig. 13. TEM and EDS analysis of 5.5 wt% NiO/olivine two-step impregnation, calcined at 1100 °C after test.

after the testing of each system are of the original olivine phase and metallic nickel. A phase resembling iron oxide was not detected. On the SEM photographs the catalysts exhibit similar characteristics both before and after testing. For example, SEM analyses following the testing of 5.5 wt% NiO on olivine calcined at 1100 °C are shown in Fig. 12. This similarity suggests that the principal effect of the catalytic test is the reduction of nickel oxide particles to the metal along with an accompanying decrease in size. For the catalyst obtained via a two-step impregnation by nickel, the change consists of a less regular distribution of the metal upon the surface. EDS analysis of this sample (Fig. 13) predicts three types of particles on the support: Ni and Ni–Fe as indicated before the test and a new species identified as iron. These new species of iron oxides are different from those free found upon the natural olivine. By impregnation of nickel, the free iron oxides from olivine react to yield Ni–Fe oxides as shown by TEM and EDS. These species correspond to a proportion of the iron previously bonded into the olivine structure: the iron of  $(\text{Mg}_{0.8}, \text{Fe}_{0.2})_2\text{SiO}_4$ .

#### 4. Discussion

Yang et al. [8] have described Ni/SiO<sub>2</sub> preparation by an impregnation of nickel nitrate and by a two-step method using a ethylene diamine salt of Ni and a nitrate salt of Ni. In Ni/SiO<sub>2</sub> prepared with simple impregnated method, the nitrate decomposes to 320 °C during the calcination step and bulk NiO particles are obtained after heating. The authors modified the preparation by the Ni(en)<sub>3</sub> given strong interaction with the silica and able to play the role of chemical glue for future addition of nickel. In the case of the olivine, the results showed that a part of nickel species is grafted on olivine by strong interaction with Si. The final system is close to Yang's one without the initial step of impregnation of Ni(en)<sub>3</sub> in the preparation. The part of the grafted Ni species increases with the temperature. Between 750 and 1100 °C, the amount of grafted Ni species is high enough to prevent the migration and growth of oxidised or reduced Ni particle. After calcination at 750, 900 and 1100 °C, the catalytic studies showed that at high temperature (at 800 °C) the yield into H<sub>2</sub> and CO are very high and stable in time. The main difference was observed by an increase of performance with temperature during the activated run in the order: Ni/olivine calcined at 750 > 900 > 1100 °C. This fact is due to the freedom of reducible NiO in relation with grafted Ni species. With a high temperature of calcination (1400 °C), NiO on olivine is particularly homogeneous as demonstrated by TEM. The NiO is integrated into the structure. In this case, clusters of iron oxides are included in the olivine

matrix giving a homogeneous appearance as shown by EDS [18].

The consequence of the exchange between iron oxides and nickel oxide into the olivine structure is both the ability of nickel to be grafted onto the surface and the decrease in the catalytic performance for the dry reforming of methane reaction. For an impregnation of a modest amount of nickel salt, the exchange results in a larger dispersion of nickel aggregates upon the surface and by the relatively large amount of iron oxides contained in the olivine structure. A part of nickel oxide is integrated into the structure and anchors the metal to the surface. These particles are maintained on the olivine by the silicate formed on the surface. In this way, the nickel reservoir masks completely the surface though it can be reduced under the testing conditions. The two-step impregnation of nickel nitrate produces a catalyst of lower stability. The initial step with 3.5 wt% of NiO on olivine favours the exchange of nickel oxide into the olivine structure. A double calcination increases progressively the migration of iron oxides to the olivine surface which leads to a decrease in the catalytic performance with time. Iron species favour the reverse water gas shift reaction:  $\text{CO}_2 + \text{H}_2 \rightarrow \text{CO} + \text{H}_2\text{O}$ . The water formed increases the oxidation of the metallic nickel to the hydroxide which is known to have a promoter effect on the exchange of iron oxides with nickel oxide into the natural olivine [19]. By addition of larger amounts of nickel with a single impregnation, it is possible to anchor nickel oxide well to the olivine surface and to limit the amount of iron oxides on the surface by a short calcination. This catalyst demonstrates an excellent performance in the dry reforming of methane.

#### 5. Conclusion

Natural olivine has good characteristics as a support for nickel catalysts. The hardness, density and basicity are useful for the gasification of biomass and compatible with its quality as support for the case described. A proportion of nickel oxide is included in the olivine and maintains the level of reducible nickel oxide. This reservoir of nickel is the active phase of the catalyst in the dry reforming of methane reaction. The parameters relating to the preparation can be controlled in order to limit the presence of free iron oxides on the surface of the catalyst and to obtain a very stable and active system for syngas formation. The CO<sub>2</sub> + CH<sub>4</sub> mixture reduces nickel oxide without modification of the olivine–nickel oxide interaction and without carbon deposit. This system is promising for the catalytic gasification of biomass to CO + H<sub>2</sub>, in fluidised bed, given its high attrition resistance and the presence of nickel particles strongly linked to the support.

## Acknowledgments

The authors are deeply grateful to M.G. Ehret for TEM experiments and for constructive discussions and to the European Community for its financial support under Joule contract JOR 3 CT 97 0196 Bio H<sub>2</sub>-FUEL. S. Brooks proofread the manuscript.

## References

- [1] H.H. Landsberg, *Energy the Next Twenty Years*, Ballinger Publishing Company, Cambridge, MA, 1979, pp. 77–90.
- [2] J. Saint-Just, J.M. Basset, J. Bousquet, G.A. Martin, *Natural gas, raw material on the future*, *La Recherche* 222 (1990) 730–738.
- [3] J. Corella, M.P. Aznar, J. Delgado, E. Aldea, *Steam gasification of cellulosic wastes in a fluidized bed with downstream vessels*, *Ind. Engng. Chem. Res.* 30 (1991) 2252–2262.
- [4] F. Winter, C. Wartha, H. Hofbauer, *NO and N<sub>2</sub>O formation during the combustion of wood, straw, malt waste and peat*, *Bioresour. Technol.* 70 (1999) 39–49.
- [5] W. Zou, R.D. Gonzalez, *The chemical anchoring of noble metal amine precursors to silica*, *Catal. Today* 15 (1992) 443–453.
- [6] K. Tohji, Y. Udagawa, S. Tanabe, T. Ida, A. Ueno, *Catalyst preparation procedure probed by EXAFS spectroscopy. 2. Cobalt on titania*, *J. Am. Chem. Soc.* 106 (1984) 5172–5178.
- [7] M. Che, L. Bonneviot, *Role of oxide surface in coordination chemistry of transition metal ions in catalytic systems*, *Pure Appl. Chem.* 60 (1988) 1369–1378.
- [8] J.C. Yang, N.G. Shul, C. Louis, M. Che, *In situ EXAFS study of the nucleation and crystal growth of Ni particles on SiO<sub>2</sub> support*, *Catal. Today* 44 (1998) 315–325.
- [9] M. Houalla, F. Delannay, I. Matsuura, B. Delmon, *Physico-chemical characterization of impregnated and ion-exchanged silica-supported nickel oxide*, *J. Chem. Soc., Faraday Trans.* 76 (1980) 2128–2141.
- [10] *Natural Bureau Standard, US Monograph* 25, 20, 71 (1984), JCPDS 34-0189.
- [11] A.M. Glazer, *Simple ways of determining perovskite structures*, *Acta Crystallogr. A* 31 (1975) 756–762.
- [12] P. Pascal, *Traité de Chimie Minérale, Tome XVII*, Masson et Cie, Paris, 1933, p. 600.
- [13] H. Provendier, C. Petit, C. Estournes, S. Libs, A. Kiennemann, *Stabilization of active nickel catalysts in partial oxidation of methane to synthesis gas by iron addition*, *Appl. Catal. A* 180 (1999) 163–173.
- [14] C. Courson, L. Udron, D. Swierczynski, C. Petit, A. Kiennemann, *Hydrogen production from biomass gasification on nickel catalysts, Tests for dry reforming of methane*, *Catal. Today* accepted.
- [15] N.P. Efyushina, A.V. Shamshurin, E.A. Zhikhareva, *Crystal-field parameters of Mn<sup>2+</sup> in Mg<sub>2</sub>SiO<sub>4</sub>:Mn<sup>2+</sup>, Mg<sub>5</sub>(SiO<sub>4</sub>)<sub>2</sub>F<sub>2</sub>:Mn<sup>2+</sup>, and Mg<sub>2</sub>SiO<sub>4</sub>:MgF<sub>2</sub>:Mn<sup>2+</sup>*, *Inorg. Mater.* 34 (1998) 514–516.
- [16] A.M. Huntz, C. Liu, M. Kornmeier, J.L. Lebrun, *The determination of stresses during oxidation of Ni: in situ measurements by XRD at high temperature*, *Corros. Sci.* 35 (1993) 989–997.
- [17] C. Courson, C. Petit, A. Kiennemann, *Physicochemical characterization of a natural olivine and its use as an industrial catalysts*, *J. Phys. IV* 10 (2000) Pr10/531–Pr10/540.
- [18] R. Blom, I.M. Dahl, A. Slagtern, B. Sortland, A. Spjelkavik, E. Tangstad, *Carbon dioxide reforming of methane over lanthanum-modified catalysts in a fluidized-bed reactor*, *Catal. Today* 21 (1994) 535–544.
- [19] P. Pascal, *Traité de Chimie Minérale, Tome X*, Masson et Cie, Paris, 1933, pp. 2–3.